

COMMUNICATION

# Crystal Structure of a T Cell Receptor V $\alpha$ 11 (AV11S5) Domain: New Canonical Forms for the First and Second Complementarity Determining Regions

Mischa Machius<sup>1</sup>, Petru Cianga<sup>2</sup>, Johann Deisenhofer<sup>1</sup>  
and E. Sally Ward<sup>2\*</sup>

<sup>1</sup>Howard Hughes Medical Institute and Department of Biochemistry, University of Texas Southwestern Medical Center, 5323 Harry Hines Blvd., Dallas, TX 75390-9050, USA

<sup>2</sup>Center for Immunology and Cancer Immunobiology Center University of Texas Southwestern Medical Center 5323 Harry Hines Blvd. Dallas, TX 75390-8576, USA

We describe the X-ray crystallographic structure of a murine T cell receptor (TCR) V $\alpha$  domain ("V $\alpha$ 85.33"; AV11S5-AJ17) to 1.85 Å resolution. The V $\alpha$ 85.33 domain is derived from a TCR that recognizes a type II collagen peptide associated with the murine major histocompatibility complex (MHC) class II molecule, I-A<sup>d</sup>. V $\alpha$ 85.33 packs as a V $\alpha$ -V $\alpha$  homodimer with a highly symmetric monomer-monomer interface. The first and second complementarity determining regions (CDR1 and CDR2) of this V $\alpha$  are shorter than the CDRs corresponding to the majority of other V $\alpha$  gene families, and three-dimensional structures of CDRs of these lengths have not been described previously. The CDR1 and CDR2 therefore represent new canonical forms that could serve as templates for AV11 family members. CDR3 of the V $\alpha$ 85.33 domain is highly flexible and this is consistent with plasticity of this region of the TCR. The fourth hypervariable loop (HV4 $\alpha$ ) of AV11 and AV10 family members is one residue longer than that of other HV4 $\alpha$  regions and shows a high degree of flexibility. The increase in length results in a distinct disposition of the conserved residue Lys68, which has been shown in other studies to play a role in antigen recognition. The X-ray structure of V $\alpha$ 85.33 extends the database of canonical forms for CDR1 and CDR2, and has implications for antigen recognition by TCRs that contain related V $\alpha$  domains.

© 2001 Academic Press

**Keywords:** T cell receptor V $\alpha$  domain; complementarity determining region; canonical form; X-ray crystallography; antigen recognition

\*Corresponding author

T cells recognize peptides bound to major histocompatibility complex (MHC) class I or class II molecules on the surface of antigen-presenting cells by virtue of their  $\alpha\beta$  T cell receptors (TCRs). The formation of the ternary complex between the TCR and peptide-MHC (pMHC) leads to a cascade of signaling events that may ultimately result in T cell activation. The TCR-pMHC complex, however, does not act as a simple on-off switch. In fact, the intracellular signals can vary in strength and dur-

ation due to the ability of a T cell to sense differences in ligand quality (reviewed by Sloan-Lancaster & Allen<sup>1</sup> and Germain & Stefanova<sup>2</sup>). Although the structural basis for the ability of the TCR to distinguish between closely related ligands is not well understood, the affinity and frequently the off-rate of the interaction with ligand is a key parameter in the outcome of the T cell:antigen-presenting cell (APC) contact.<sup>3–8</sup> The effect of the off-rate on the extent of TCR triggering has led to the suggestion that TCRs need sufficient time to form a signaling competent configuration. This process may also involve the recruitment of co-receptors and other accessory molecules.<sup>9–11</sup> In addition, a recent kinetic segregation model in which the TCR-pMHC interaction results, through steric effects, in segregation of the TCR into the pro-signaling environment (e.g. phosphatase depleted) of close T cell:APC contact zones is

Abbreviations used: TCR, T cell receptor; CDR, complementarity determining region; pMHC, peptide-MHC; APC, antigen presenting cell; V, variable; CII, type II collagen; HV, hypervariable; MAD, multiple anomalous dispersion; MHC, major histocompatibility complex.

E-mail address of the corresponding author: [sally@skylab.swmed.edu](mailto:sally@skylab.swmed.edu)

**Table 1.** Data collection, phasing and refinement statistics

		Native	SeMet			
			11	12	13	14
<i>A. Data collection</i>						
Energy (eV)			11,500	12,661	12,663	13,100
Unit cell (Å)	<i>a=b</i>	83.6			83.5	
	<i>c</i>	132.3			132.1	
Resolution (Å)		1.85	2.00	2.00	2.00	2.00
Completeness						
	Overall (%)	98.7	98.5	99.9	99.9	99.9
	Last shell (%)	97.9	90.5	99.6	93.7	99.9
$R_{\text{merge}}^a$						
	Overall (%)	4.4	9.9	10.7	10.3	11.5
	Last shell (%)	54.1	47.9	83.7	78.2	66.3
$I/\sigma(I)$						
	Overall	30.8	16.5	15.5	16.8	14.8
	Last shell	3.1	2.1	1.6	1.7	2.4
Multiplicity						
	Overall	6.5	10.3	11.1	11.2	11.2
	Last shell	5.7	4.6	7.8	8.1	10.6
<i>B. MAD phasing</i>						
Number of sites				8		
Resolution (Å)				40.0-2.25		
Phasing power			1.25	-	0.72	1.29
Figure of merit				0.49		
<i>C. Refinement</i>						
Resolution range (Å)			33.5-1.85			
Reflections						
working set			41,791			
free set			2189			
Completeness (%)			95.0			
$\sigma$ -Cutoff			0.0			
Atoms in model						
Protein (non-hydrogen)			3535			
Chloride			3			
Glycerol			18			
Water			266			
Refinement parameters						
$R_{\text{work}}$			0.219			
$R_{\text{free}}$			0.236			
Average atomic displacement parameters (Å <sup>2</sup> )						
Protein			36.3			
Chloride			26.8			
Glycerol			63.8			
Water			51.6			
Deviations from ideality						
Bond lengths (Å)			0.012			
Bond angles (deg.)			1.42			
Dihedral angles (deg.)			24.56			
Improper angles (deg.)			1.28			

<sup>a</sup>  $R_{\text{merge}} = \sum_h \sum_i |I_{h,i} - \langle I_h \rangle| / \sum_h \sum_i I_{h,i}$ , where the outer sum ( $h$ ) is over the unique reflections and the inner sum ( $i$ ) is over the set of independent observations of each unique reflection.

consistent with the correlation between TCR-pMHC stability and signaling outcome.<sup>12</sup>

Major steps towards reaching an understanding of T cell recognition have been made with the determination of structures of TCRs complexed with cognate pMHC class I or class II ligands.<sup>13-21</sup> For TCR-pMHC class I complexes, these studies revealed that the TCR docks in a diagonal mode on cognate ligand, with the third complementarity determining regions (CDR3s) of the TCR playing a central, plastic role in peptide recognition. However, in the TCR-pMHC class I complexes with known structure there is considerable variability in the "twist angle" (45-70°) of the TCR with respect

to its ligand. The first report of the solved structure of a TCR bound to cognate pMHC class II revealed that in this case the TCR is oriented in an almost orthogonal orientation (80°) relative to the pMHC ligand.<sup>18</sup> The different configurations of TCRs on pMHC class I and class II ligands were suggested to have implications for the selection of T cells into the CD4 or CD8 lineage during thymic development.<sup>18</sup> However, more recent structural studies of an HLA-DR1-restricted TCR show that the TCR is oriented at an angle of 70°,<sup>20</sup> which falls at the upper end of the range reported for MHC class I restricted TCRs.<sup>13-17</sup> Although the TCR-pMHC class II complexes appear to have twist angles at

the higher end of the range, for MHC class I and class II restricted complexes the CDR footprint on the cognate ligand is approximately diagonal for both types of interaction.<sup>22</sup> Furthermore, nearly all ternary complexes analyzed to date share the feature that a greater number of contacts with the cognate pMHC ligand are made by the V $\alpha$  domain than by the V $\beta$  domain of the TCR (reviewed by Garcia *et al.*<sup>23</sup> with the exception of a TCR-alloligand complex.<sup>21</sup> The dominance of the V $\alpha$  domain in the interactions is consistent with studies indicating a role for this region of the TCR in affecting the outcome of thymic selection.<sup>24–26</sup>

Much attention has focussed on the V $\alpha$  and V $\beta$  domains of TCRs, because they ultimately determine the specificity of T cell recognition. Despite the fact that there are only a few high-resolution structures known for TCR V $\alpha$  and V $\beta$  domains, a number of characteristic features are recognizable. Most strikingly, V $\alpha$  domains either complexed with ligand or in the uncomplexed form have an unusual strand topology when compared with the structurally very similar immunoglobulin V domains.<sup>13–21,23,27–31</sup> The V $\alpha$  strand topology involves the switching of the C' strand (fifth  $\beta$ -strand) to pair with the D strand rather than with the C' strand,<sup>27</sup> as observed in immunoglobulins. The V $\beta$  domain strand topology is generally immunoglobulin V domain-like, although in the KB5-C20 and BM3.3 TCRs (both V $\beta$ 2) it adopts the V $\alpha$  strand topology<sup>21,29</sup> and an intermediate conformation is seen in the D10 TCR.<sup>30</sup> The altered topology of V $\alpha$  domains is a consequence of a flipping of the C' strand from the inner to the outer  $\beta$ -sheet, which results in a rotation of CDR2 by about 90° to form a more compact binding site (reviewed by Garcia *et al.*<sup>23</sup>). Insertion of a potential glycosylation site in the region encompassing the C' strand of the 1934.4 V $\alpha$  domain has differential effects on T cell activation events.<sup>32</sup> This suggests that the flatter surface of the V $\alpha$  domain introduced by the C' strand flip in this region has functional significance.

Understanding T cell responses at an atomic level requires detailed characterization of structures of TCR V domains. However, structural information is available only for a limited number of TCR V domains and they represent an even more limited number of gene families.<sup>13–21,27–31,33</sup> The availability of a greater number of TCR structures is necessary to define canonical forms for the CDRs. A similar analysis for immunoglobulins, where dozens of three-dimensional structures have been determined, proved to be seminal for understanding their function. Indeed, a very recent comparison of the available TCR V domain structures indicates that the CDRs do in fact share some similarities from one TCR to another, but there are also significant variations for TCR V regions of different Kabat subgroups.<sup>34</sup> Since TCRs do not undergo somatic mutation, the structures corresponding to individual V gene families should provide templates for all other TCRs that share the same V

gene. Thus, there is a need to generate a library of structures so that an assessment of the regions of structural variability and similarity from one TCR to the next can be made. Such an analysis will also increase the accuracy with which the structures of TCRs can be predicted and modeled.

In the current study we describe the three-dimensional structure to 1.85 Å resolution of a murine V $\alpha$  domain (V $\alpha$ 85.33; AV11S5-AJ17) derived from a TCR that recognizes the immunodominant epitope of type II collagen (CII) associated with the MHC class II molecule I-A<sup>a</sup>.<sup>35</sup> This TCR was isolated from an autoreactive T cell clone associated with the mouse model of arthritis, collagen induced arthritis.<sup>36</sup> Analysis of the response to CII indicates that AV11 family members are present in about 50% of the CII-specific T cells,<sup>37</sup> and structural knowledge concerning the V $\alpha$ 85.33 domain is therefore relevant to understanding autoantigen recognition in this murine disease model. The structure of this V $\alpha$  domain, for which the V region is a member of the AV11S5 sub-family,<sup>35,38</sup> is also of interest, as the CDR1 and CDR2 lengths are shorter than in the majority of TCRs.<sup>38,39</sup> The shorter CDR1 and CDR2 lengths are common to other members of the AV11 family despite considerable sequence polymorphisms in these regions. In addition, expression of the AV11S1 gene family, which is closely related to AV11S5, has been shown to predispose T cells towards positive selection by MHC class II molecules and, as a result, skewing into the CD4 subset.<sup>25</sup> The CDR1 and CDR2 sequences of V $\alpha$ 85.33 are the same as those of the AV11S1 family with the exception of replacement of an alanine residue by a serine residue at position 31 in CDR1. These similarities indicate that V $\alpha$ 85.33 (or its close homologs) may have a preference for recognizing MHC class II molecules over MHC class I molecules, a feature for which the structural basis is not yet fully understood.

V $\alpha$ 85.33 crystallized with the symmetry of space group  $P3_221$  with four molecules in the asymmetric unit. Crystals of V $\alpha$ 85.33 diffracted well to better than 1.85 Å Bragg spacing when using synchrotron radiation. Attempts to solve the crystal structure of V $\alpha$ 85.33 by molecular replacement with known structures of V $\alpha$  domains and immunoglobulins as search models failed, possibly because of the relatively large number of molecules per asymmetric unit and the high-symmetry space group. We therefore solved the V $\alpha$ 85.33 crystal structure using multiple anomalous dispersion from seleno-methionine. The quality of the phases obtained from the selenium atoms was sufficient for structure solution, although the two methionine residues per molecule were not well ordered. Furthermore, diffraction spots at high resolution had a smeary appearance indicating disorder in the crystal. The quality of the electron density for the four molecules differs somewhat. In addition to several side-chains in loop regions of the four monomers, four residues in the HV4 region and four residues

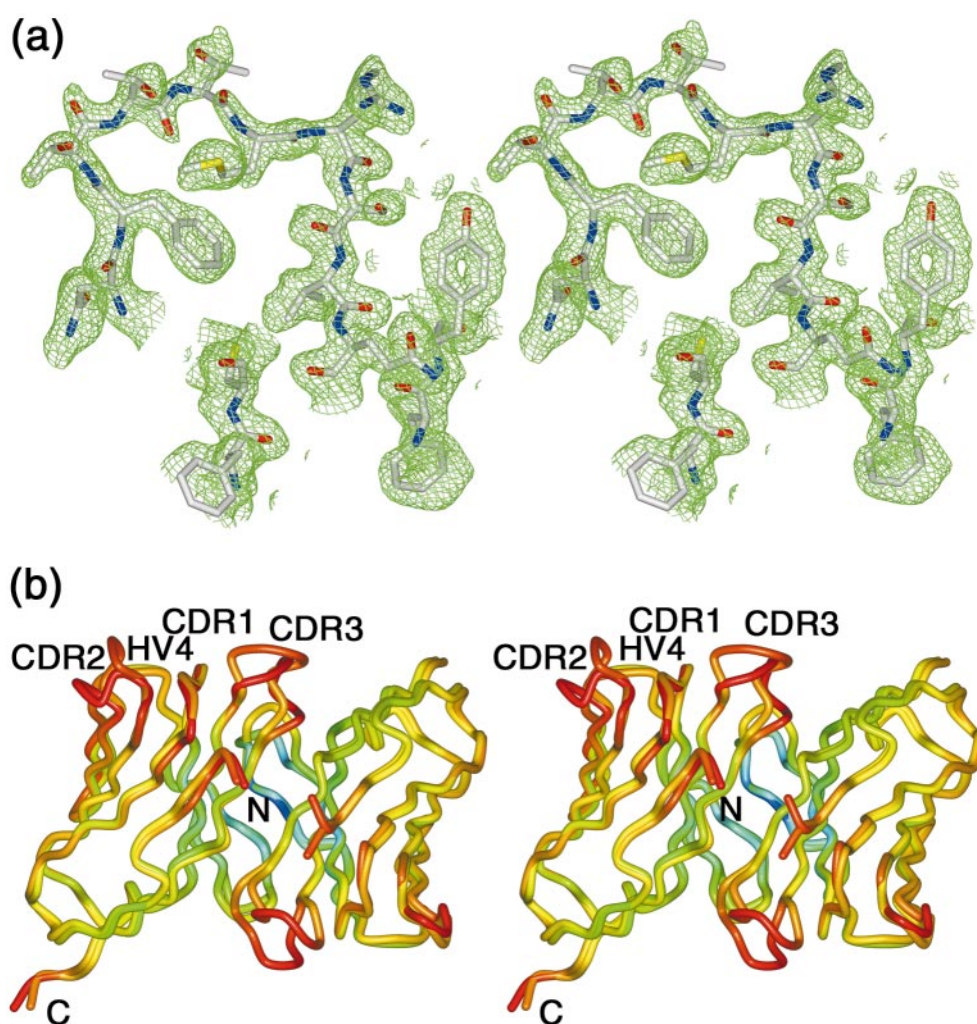


Figure 1 (legend opposite)

in the CDR3 loop of monomer A are poorly defined. Analysis of the atomic displacement parameters shows that monomers C and D are best ordered (mean  $B$ -factor = 33.8 Å<sup>2</sup> and 33.5 Å<sup>2</sup>, respectively), with the mean  $B$ -factor for monomers A and B being 4 and 7 Å<sup>2</sup> higher. The N-terminal region of monomer A appears to be substantially disordered, although the same region is well defined in the other monomers.

The overall structure of V $\alpha$ 85.33 is typical for TCR V $\alpha$  domains (Figure 1). The core consists of two sets of antiparallel  $\beta$ -strands connected by loops of varying lengths and structure. The four V $\alpha$ 85.33 molecules (A, B, C, and D) in the asymmetric unit form two homodimers (AB and CD). The V $\alpha$ 85.33 dimers are distinct from those reported previously<sup>27,28</sup> because the V $\alpha$  monomers are packed "head-to-tail" so that their CDRs point in opposite directions. The structures of the V $\alpha$ 85.33 monomers are very similar within a dimer, with rmsd for the C $\alpha$  positions in the core region of 0.35 Å for the dimer AB and 0.29 Å for

the dimer CD. However, they show larger differences when compared to monomers from the other dimer (rmsd = 0.73 - 0.80 Å). Generally, the interface in V $\alpha$ :V $\alpha$  homodimers is based on shape complementarity involving mostly hydrophobic interactions and a few polar interactions. The V $\alpha$ 85.33 monomer-monomer interface is highly symmetric and involves identical residues at similar positions in both chains. Three regions contribute to the interface: around residue 9, around residue 40, and around residue 103. The center of the 2-fold symmetry axis relating the two monomers is formed by a double main chain-main chain hydrogen bond between opposing Leu43 flanked by hydrogen bonds between Ser42OG of one monomer and Ser45N of the other. As the V $\alpha$ 85.33 monomers form a dimer with an unusual configuration, the nature of the monomer-monomer packing does not have relevance to physiological V $\alpha$ :V $\beta$  dimers.

The core region of the V $\alpha$ 85.33 domain structure superimposes very well with both murine and



human V $\alpha$  domains of known three-dimensional structure (Figure 2). The structurally closest relative is the human TCR A6,<sup>14</sup> with an rmsd for the core region of 1.10 Å (1.27 Å overall). With the slowly accumulating number of three-dimensional structures available for V $\alpha$  domains, features that are common to all V $\alpha$  domains and features that are specific for a given family start to emerge. For example, previously unnoted is the fact that the N-terminal region between residues 5 and 10, which precede and are part of  $\beta$ -strand A, adopts three different classes of conformations in the V $\alpha$  structures. V $\alpha$ 85.33, together with KB5-C20, D10, B4.2.3, and HA1.7, form one family of structures, A6, N15 and 1934.4 form a second family, and 2C, B7 and BM3.3 form a third. A second feature is that, within  $\beta$ -strand B, V $\alpha$ 85.33 deviates substantially at position 18 from any other TCR structure. Ser18 in V $\alpha$ 85.33 has mean main chain torsion angles of  $\phi = -154(\pm 2)^\circ$  and  $\psi = 168(\pm 5)^\circ$  (averaged over the four molecules in the asymmetric unit of our crystal form) compared to  $\phi = 120(\pm 12)^\circ$  and  $\psi = 135(\pm 12)^\circ$  for the other TCRs. The conformation of this region is not influenced by crystal contacts but is an inherent feature of V $\alpha$ 85.33. The most striking structural differences in the core region of V $\alpha$  domains, however, occur in the C'-D  $\beta$ -hairpin. A6, B4.2.3, B7, D10, KB5-C20 and BM3.3

form one class, 2C, 1934.4, N15 and HA1.7 form another class. V $\alpha$ 85.33 shows a mixed mode conformation with the base of the hairpin belonging to the first class and the remainder belonging to the second class. Finally, a fourth structurally diverse spot exists around residue 78, with 1934.4, HA1.7 and 2C, KB5-C20 and B7, and A6, B4.2.3, D10, BM3.3 and V $\alpha$ 85.33 forming distinct families. These four structural features of the core region are well defined. However, they do not seem to be characteristic for a given TCR family, nor can they be attributed to the fact that in some of the known structures the V $\alpha$  domain is in complex with cognate pMHC ligand, whereas in others it is solitary. There are still too few structural and functional studies for V $\alpha$  domains to allow a correlation between these characteristics and physiological processes to be made.

The specificity of the interaction between a TCR and the corresponding pMHC complex is determined primarily by residues located in the CDRs. For CDRs 1 and 2 of both TCR  $\alpha$  and  $\beta$ -chains, sets of canonical structures have been defined.<sup>34</sup> V $\alpha$ 85.33 is distinct from the V $\alpha$  domains for which three-dimensional structures are available, in that CDR1 and CDR2 are shorter than those found in the majority of other TCR V $\alpha$  families.<sup>38,39</sup> For example, mouse AV10 is the only other V $\alpha$  family

**Figure 1.** Stereo Figure of the structure of V $\alpha$ 85.33. (a)  $2F_o - F_c$  omit map in the region around CDR1. (b) Superposition of the C $^\alpha$  backbone traces of the two V $\alpha$ 85.33 dimers in the asymmetric unit. The backbone is colored according to atomic displacement parameters (blue = 18 Å<sup>2</sup>, red = 100 Å<sup>2</sup>). Superpositions were done with the program SPDBViewer.<sup>50</sup> The complementarity determining regions, the fourth hypervariable region (HV4) as well as the C and N termini are indicated. All Figures were generated with Bobscrip<sup>51</sup> gl\_render (L. Esser, University of Texas Southwestern Medical Center, unpublished) and PovRay (Persistence of Vision Ray Tracer, v3.02, POV-Team, [www.povray.org](http://www.povray.org)). Methods: the V $\alpha$ 85.33 domain containing a His<sub>6</sub>-tag was expressed as a secreted protein in *Escherichia coli* as described.<sup>35</sup> Crystals were obtained at 20 °C by vapor diffusion from drops containing 3  $\mu$ l of protein (5 mg ml<sup>-1</sup> in 50 mM Tris-HCl (pH 8.0), 100 mM NaCl) plus 3  $\mu$ l of reservoir solution (100 mM sodium citrate-HCl, 1.4-1.7 M lithium chloride, pH 5.0-6.0) equilibrated against 1 ml of reservoir solution. Hexagonal crystals appeared after three to ten days and grew to a final size of 0.7 mm diameter and 0.3 mm thickness within one to three weeks. V $\alpha$ 85.33 crystallized with the symmetry of space group P3<sub>2</sub>21 with cell constants of  $a = b = 83.5$  Å,  $c = 132.1$  Å, and four molecules per asymmetric unit. Prior to data collection, the crystals were cryo-protected by transferring them into harvesting solution (100 mM sodium citrate-HCl, 2 M lithium chloride, pH 5.5) supplemented with up to 40% (v/v) glycerol and flash-cooled in liquid propane. The crystals diffracted to 1.85 Å Bragg spacing when using synchrotron radiation. The structure was solved by multiple anomalous dispersion (MAD) using a seleno-methionine variant (two methionine residues per molecule). The seleno-methionine variant of V $\alpha$ 85.33 was expressed in the methionine-auxotroph *E. coli* strain B834 grown in minimal medium supplemented with the natural amino acids and seleno-methionine. Purification and crystallization behavior was essentially unchanged compared to native V $\alpha$ 85.33. The MAD experiment was carried out at beamline 19-ID (SBC-CAT) at the Advanced Photon Source (Argonne National Laboratory, Argonne, Illinois, USA). Data were indexed, integrated and scaled with the HKL2000 program package.<sup>52</sup> Eight selenium sites were identified at 2.5 Å resolution by direct methods (Shake'n'Bake 2.0<sup>53</sup>) using the data set collected at the energy for the selenium absorption peak. Selenium parameters were refined and the resulting phases (figure of merit 0.49) were improved by density modification using programs from the CCP4 package,<sup>54</sup> resulting in a figure of merit of 0.69. Model building was done with the program O.<sup>55</sup> Structure refinement was carried out with the program CNS v0.5<sup>56</sup> employing cycles of simulated annealing, conjugate gradient minimization and calculation of individual atomic displacement parameters. Calculation of overall anisotropic displacement parameters and bulk solvent correction was used throughout. No non-crystallographic symmetry restraints were used at the highest resolution (1.85 Å). Water molecules were added where stereochemically reasonable after the protein part was completed. Side-chains with poorly defined density were truncated to alanine for refinement purposes. The final model contains residues 2 to 112 for molecule 1, residues 2 to 110 for molecule 2, residues 2 to 112 for molecule 3, residues 2 to 110 for molecule 4, three chloride ions, three glycerol molecules and 266 water molecules. The correctness of the model was confirmed through simulated annealing omit maps. The  $R_{\text{free}}$  value is 23.6% and the  $R_{\text{work}}$  value is 21.9% (Table 1).

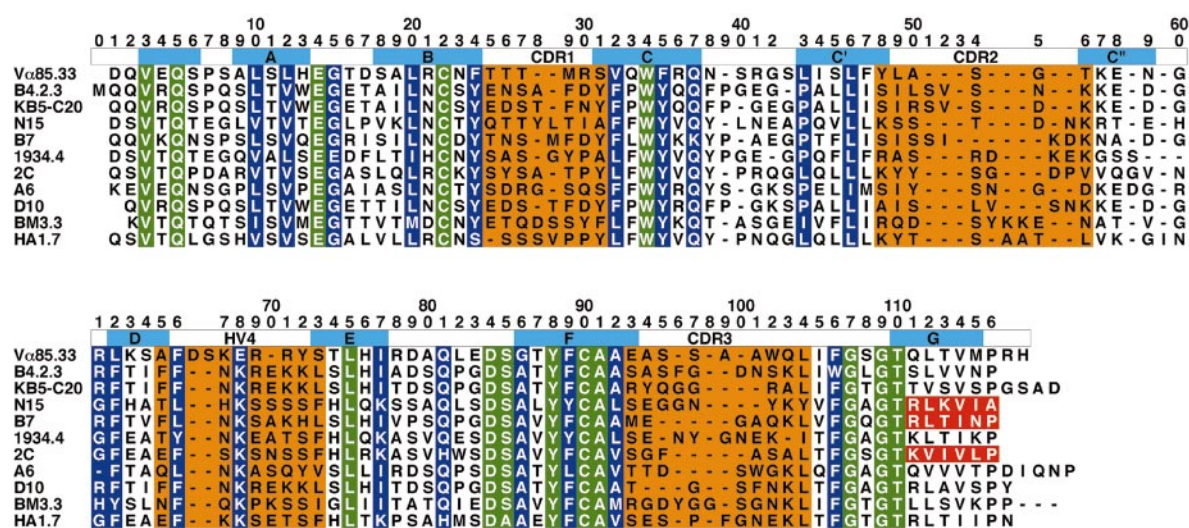


**Figure 2.** Structure-based sequence alignment of TCR V $\alpha$  domains of known three-dimensional structure. The superposition is based on PDB entry 1b88 for B4.2.3, 1tcr for 2C, 1nfd for N15, 1bd2 for B7, 1kb5 for KB5-C20, 1ao7 for A6, 1d9k for D10, 1f0o for BM3.3, 1fty for HA1.7, and Fields *et al.*<sup>27</sup> for the 1934.4 V $\alpha$ . The sequence numbering is according to Kabat *et al.*<sup>39</sup> Gaps in the numbering scheme occur at positions where the structure-based sequence alignment does not match the pure sequence alignment. CDR boundaries are according to Chothia *et al.*<sup>57</sup> Strictly conserved residues are shown in green, highly conserved residues in blue, and residues that are not observed in the crystal structures in red. The CDRs and the fourth hypervariable region (HV4) are shown in orange. The central  $\beta$ -strands are marked with cyan bars.

that has CDR1 and CDR2 of the same length.<sup>38</sup> The structures of the V $\alpha$ 85.33 CDR1 and CDR2 loops might therefore be expected to give rise to new canonical forms that can be used as a template for these shorter CDRs.

For CDR1 $\alpha$ , three canonical structures have been defined to date.<sup>34</sup> These canonical structures contain nine or ten residues and show a characteristic residue packing. Compared with V $\alpha$ 85.33, all other V $\alpha$  CDR1 regions have an insertion after residue 27, or, in order to obey the established residue numbering scheme, residue 28 is missing from V $\alpha$ 85.33. In its overall structure, V $\alpha$ 85.33-CDR1 is reminiscent of the canonical structure  $\alpha$ 1-1 found in A6, KB5-C20, D10 and B7 (Figure 3(a)). However, there are several features that clearly distinguish the conformation of V $\alpha$ 85.33-CDR1 from the  $\alpha$ 1-1 canonical form. First, the key residues are Phe at position 24 (as opposed to Tyr in the other TCRs), Met at position 29 (as opposed to either Ser or Phe), and Val at position 32 (as opposed to Phe). Second, as a consequence of the shorter and therefore tighter loop, the side-chains of key residues 24 and 32 in V $\alpha$ 85.33 are rotated by about 120° and 180°, respectively, when compared to the  $\alpha$ 1-1 canonical form. They point towards the interior of the protein, a packing scheme that is not found in any other CDR1 $\alpha$  structure. As noted by Al-Lazikani *et al.*,<sup>34</sup> the variation in the size of key residue side-chains (particularly at position 29) is highly unusual for conserved compact structures. Nevertheless, it appears that tight and stable packing can be achieved in all cases. Finally, there are no hydrogen bonds stabilizing the CDR1 region in V $\alpha$ 85.33. Taken together, V $\alpha$ 85.33 contains a new

canonical form for TCR-CDR1 $\alpha$  regions that we propose to call  $\alpha$ 1-4. The key packing residues for CDR1 $\alpha$ s in the seven subgroups of AV11 are reasonably well conserved with the exception of Met29, which is usually Thr or Ala.<sup>38</sup> This indicates that the  $\alpha$ 1-4 canonical form will serve as a template for all AV11 family members. However, although the AV10 CDR1 is of the same length as that of AV11, in nearly all subgroups, Met29 is replaced by Leu, Thr or Ala and Val32 is replaced by Met or Leu (with the exception of AV10S3 which has Val).<sup>38</sup> This divergence of sequence at key positions suggests that the  $\alpha$ 1-4 canonical form may not be representative for this region of AV10 TCRs.

CDR2 connects the C' strand with the C'' strand. In the TCRs with known structures, there are three or four residues in the CDR2 $\alpha$  loop between the key framework residues 48 and 56. Four different canonical forms ( $\alpha$ 2-1 to  $\alpha$ 2-4) have been described for this region.<sup>38</sup> V $\alpha$ 85.33 contains only two residues in the CDR2 loop (Figure 3(b)). In V $\alpha$ 85.33, Leu49 is the key residue that forms the base of the CDR2 $\alpha$  loop, with the following two residues folding around its side-chain. The CDR2 $\alpha$  loop is virtually flat with  $\phi/\varphi$  angles (in degrees) for the loop residues Leu49 -136(10)/135(8), Ala50 -107(±5)/-16 ± 6, Ser54 -179 ± 7/174 ± 8, and Gly55 63 ± 6/-145 ± 3 (standard deviations in parentheses are based on the four molecules in the asymmetric unit). The CDR2s are stabilized by interactions with framework residues 32 and 66 and therefore interact with the CDR1 loops. Residues 32 and 66 are a pair of Phe/Leu (in N15, B7, and A6), Phe/Phe (in B4.2.3, KB5-C20, and D10),



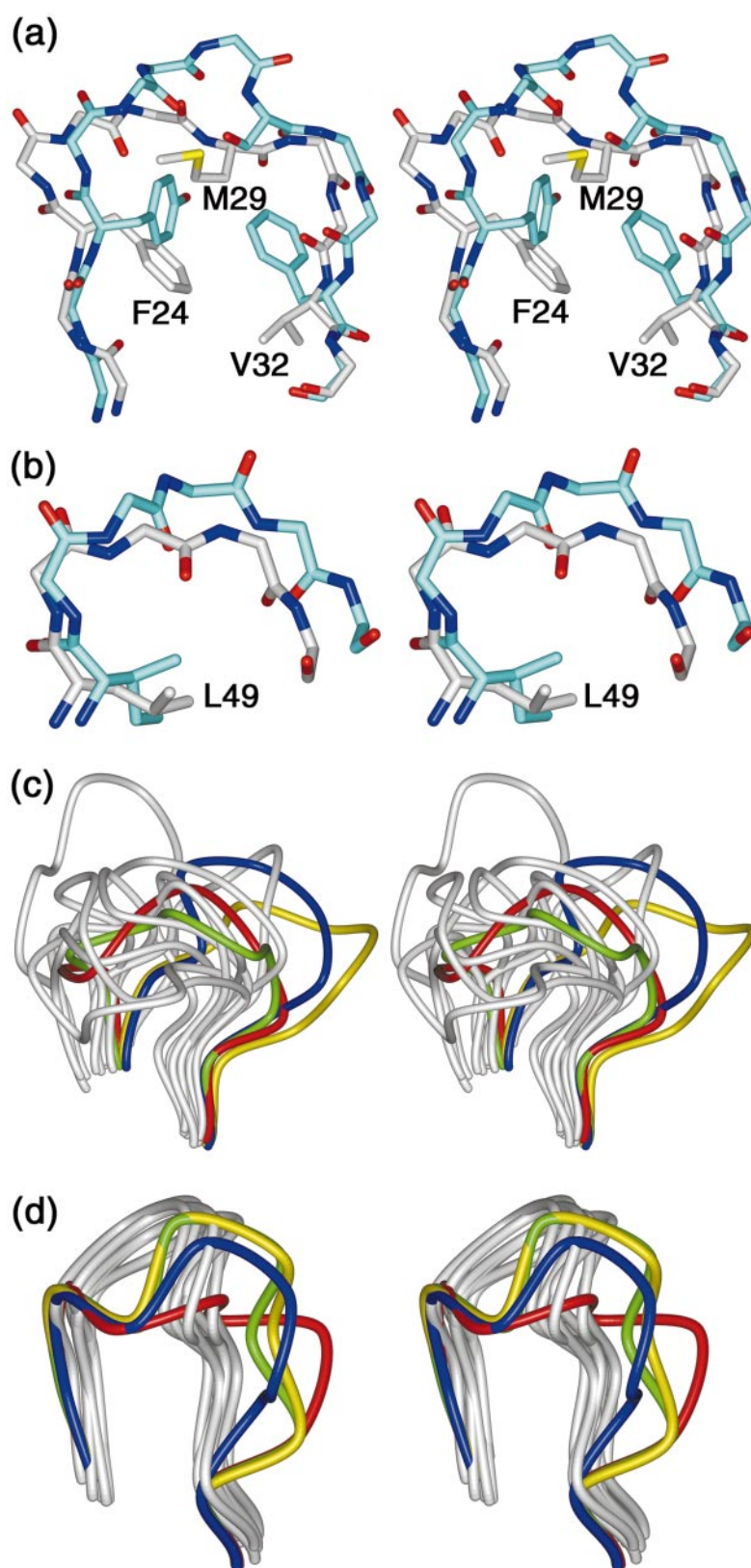


**Figure 3.** Stereo figures of the complementarity determining regions (CDRs) and the fourth hypervariable region (HV4). (a) CDR1 of  $V\alpha 85.33$  (carbon atoms are shown in gray) superimposed on the CDR1 of A6 (carbon atoms are shown in cyan). (b) CDR2 of  $V\alpha 85.33$  (carbon atoms are shown in gray) superimposed on the CDR2 of A6 (carbon atoms are shown in cyan). (c) The backbone of the  $V\alpha 85.33$ -CDR3 regions of all four molecules in the asymmetric unit (colored in red, green, blue and yellow) superimposed on the CDR3 regions of A6, TCR, B.4.2.3, KB5, N15-C20, B7, BM3.3, HA1.7, and 1934.4 (colored in gray). (d) The backbone of the  $V\alpha 85.33$ -HV4 regions of all four molecules in the asymmetric unit (colored in red, green, blue and yellow) superimposed on the HV4 regions of A6, TCR, B.4.2.3, KB5, N15, B7, D10, BM3.3, HA1.7, and 1934.4 (colored in gray).

Leu/Phe (in 2C, HA1.7 and BM3.3) and Leu/Tyr in 1934.4. In  $V\alpha 85.33$  they are Val/Phe. The conformation of  $V\alpha 85.33$ -CDR2 constitutes a new canonical form for this region, which we designate  $\alpha 2-5$ .

The fact that Val32, Leu49 and Phe66 are conserved in the AV11 subgroups<sup>38</sup> suggests that the  $\alpha 2-5$  conformation is a template for all AV11 members. In contrast, these residues are not well con-

served in any of the AV10 subgroups,<sup>38</sup> indicating that CDR2 of this TCR V $\alpha$  family has a distinct canonical form.

In contrast to CDR1 $\alpha$  and CDR2 $\alpha$ , no canonical structures have been described for the CDR3 $\alpha$  loops because of their varied lengths (six to 12 residues) and divergent sequences.<sup>39</sup> In all known TCR structures, the CDR3 loops are generally less well defined and adopt different conformations, suggesting that these regions of the TCR are highly flexible. In V $\alpha$ 85.33, CDR3 adopts different structures in the four molecules within the asymmetric unit (Figure 3(c)). This region is characterized by comparatively weak electron density. CDR3 in molecule B is not involved in crystal contacts and can therefore be considered the intrinsic conformation of this region. However, as noted earlier,<sup>27</sup> the flexibility and conformation of this region of the TCR may be different when CDR3 $\alpha$  is packed against CDR3 $\beta$  in the "native" TCR heterodimer. CDR3 of molecule B shows the highest flexibility as judged by the atomic displacement parameters. Its conformation is most similar to the equivalent region in B7.<sup>16</sup> In general, the CDR3 $\alpha$ s in the TCRs with known structure have a similar disposition (Figure 3(c)), except when crystal contacts influence their conformation. This structural variation can be observed in V $\alpha$ 85.33, where the CDR3s of molecules A, C, and D are, to varying degrees, in contact with symmetry-related molecules. Flexibility of both CDR3 $\alpha$  and CDR3 $\beta$  appears to be required for antigen recognition, in which these loops play central roles.<sup>14–18,40,41</sup> Indeed, this region of the TCR appears to undergo conformational adjustments to accommodate different peptide ligands<sup>17,19</sup> and in an NMR study has been shown to be highly mobile.<sup>30</sup> The extent of complementarity achieved by CDR3 rearrangement has been proposed to affect the functional outcome of the TCR-pMHC interaction.<sup>17,19</sup> As a consequence, the TCR is remarkably sensitive to minor changes in peptide ligand. Consistent with structural data indicating a role for induced fit in TCR-pMHC interactions,<sup>14,15,17,19</sup> binding is accompanied by unfavorable entropic changes that are compensated for by favorable enthalpic changes.<sup>42–44</sup> The characteristic features of TCR recognition, which include low affinity and an ability to "scan and adjust" to ligands, most likely contributes to the high cross-reactivity that is observed for TCRs (reviewed by Mason,<sup>45</sup> Oldstone,<sup>46</sup> and Gran *et al.*<sup>47</sup>).

In addition to the V $\alpha$  CDRs, a fourth hypervariable loop (HV4) encompassing residues 65–73 has been shown in both functional and structural studies to play a role in antigen recognition.<sup>14,18,22,48</sup> In all TCR structures reported to date, this loop region contains nine residues and adopts similar conformations (Figure 3(d)). In contrast, V $\alpha$ 85.33-HV4 contains ten residues and exhibits varying conformations in the four molecules in the asymmetric unit. The same HV4 length is also seen in AV10 family members.<sup>38</sup> This region of V $\alpha$ 85.33 is

characterized by comparatively high atomic displacement parameters and missing electron density for some of the side-chains. Of the four molecules, HV4 in molecule B is not involved in crystal contacts and can therefore be considered the intrinsic conformation. In molecule D, HV4 is involved in crystal contacts, but nevertheless adopts a conformation similar to that of the intrinsic form. In contrast, the HV4 regions in molecules A and C are influenced more or less strongly by crystal contacts. Taken together, these structural features suggest that HV4 of V $\alpha$ 85.33 is characterized by a high intrinsic plasticity, similar to CDR3. Thus, this region of the TCR could contribute further to the unfavorable entropic forces that appear to be a feature of TCR-pMHC interactions.<sup>42–44</sup> HV4 residues have been suggested to influence selection of thymocytes into the CD4 or CD8 lineage.<sup>49</sup> In support of this, a conserved HV4 $\alpha$  residue, Lys68, has been proposed to orient the TCR on cognate pMHC by establishing a salt-bridge with a conserved MHC class I (Glu166 $\alpha$ 2) or class II residue (Asp76 $\alpha$ 1) (18,22). However, in the AV10 and AV11 families, this lysine residue is shifted by one amino acid position due to the slightly longer HV4, and in V $\alpha$ 85.33 this results in a different disposition of this residue (Figures 2 and 3(d)). In the absence of structural information for V $\alpha$ 11-containing TCR(s) in complex with cognate pMHC ligand(s), the functional consequences of these features of HV4 are uncertain.

In conclusion, the structure of a V $\alpha$  domain (AV11S5-AJ17) derived from an MHC class II restricted TCR is described. The core region of this V $\alpha$  domain shows the characteristic switch of the C' strand to form the A topology and superimposes closely on V $\alpha$  domains of known structure. The V $\alpha$ 85.33 CDR1 and CDR2 loops are shorter than those of other V $\alpha$  domains described to date, and their structure gives rise to new canonical forms for these regions of the TCR. These canonical structures should serve as templates for other members of the AV11 family. Finally, CDR3 and HV4 of V $\alpha$ 85.33 show a high degree of flexibility, a feature that is consistent with the concept that TCR-pMHC interactions are characterized by conformational rearrangements and unfavorable entropic forces.<sup>15,17,19,42–44</sup>

#### Protein Data Bank accession code

The coordinates have been deposited in the RCSB Protein Data Bank with accession code 1h5b.

#### Acknowledgments

Use of the Argonne National Laboratory Structural Biology Center beamlines at the Advanced Photon Source was supported by the US Department of Energy, Office of Biological and Environmental Research, under Contract no. W-31-109-ENG-38. The authors thank



Z. Otwinowski for excellent assistance with data collection. This work was supported by grants from the National Institutes of Health (R55 AR45211, R01 AI42949; E.S.W.), Arthritis Foundation (E.S.W.) and Howard Hughes Medical Institute (J.D.).

## References

- Sloan-Lancaster, J. & Allen, P. M. (1996). Altered peptide ligand-induced partial T cell activation: molecular mechanisms and role in T cell biology. *Annu. Rev. Immunol.* **14**, 1-27.
- Germain, R. N. & Stefanova, I. (1999). The dynamics of T cell receptor signaling: complex orchestration and the key roles of tempo and cooperation. *Annu. Rev. Immunol.* **17**, 467-522.
- Matsui, K., Boniface, J. J., Steffner, P., Reay, P. A. & Davis, M. M. (1994). Kinetics of T-cell receptor binding to peptide/I-E<sup>k</sup> complexes: correlation of the dissociation rate with T-cell responsiveness. *Proc. Natl Acad. Sci. USA*, **91**, 12862-12866.
- Lyons, D. S., Lieberman, S. A., Hampl, J., Boniface, J.J., Chien, Y., Berg, L. J. & Davis, M. M. (1996). A TCR binds to antagonist ligands with lower affinities and faster dissociation rates than to agonists. *Immunity*, **5**, 53-61.
- Alam, S. M., Travers, P. J., Wung, J. L., Nasholds, W., Redpath, S., Jameson, S. C. & Gascoigne, N. R. (1996). T-cell-receptor affinity and thymocyte positive selection. *Nature*, **381**, 616-620.
- Kersh, G. J., Kersh, E. N., Fremont, D. H. & Allen, P. M. (1998). High- and low-potency ligands with similar affinities for the TCR: the importance of kinetics in TCR signaling. *Immunity*, **9**, 817-826.
- Rabinowitz, J. D., Beeson, C., Lyons, D. S., Davis, M. M. & McConnell, H. M. (1996). Kinetic discrimination in T-cell activation. *Proc. Natl Acad. Sci. USA*, **93**, 1401-1405.
- McKeithan, T. W. (1995). Kinetic proofreading in T-cell receptor signal transduction. *Proc. Natl Acad. Sci. USA*, **92**, 5042-5046.
- Hampl, J., Chien, Y. & Davis, M. M. (1997). CD4 augments the response of a T cell to agonist but not to antagonist ligands. *Immunity*, **7**, 379-385.
- Madrenas, J., Chau, L. A., Smith, J., Bluestone, J. A. & Germain, R. N. (1997). The efficiency of CD4 recruitment to ligand-engaged TCR controls the agonist/partial agonist properties of peptide-MHC molecule ligands. *J. Exp. Med.* **185**, 219-229.
- Madrenas, J. & Germain, R. N. (1996). Variant TCR ligands: new insights into the molecular basis of antigen-dependent signal transduction and T cell activation. *Semin. Immunol.* **8**, 83-101.
- van der Merwe, A., Davis, S. J., Shaw, A. S. & Dustin, M. L. (2000). Cytoskeletal polarization and redistribution of cell-surface molecules during T cell antigen recognition. *Semin. Immunol.* **12**, 5-21.
- Garcia, K. C., Degano, M., Stanfield, R. L., Brunmark, A., Jackson, M. R. & Peterson, P. A. *et al.* (1996). An  $\alpha\beta$  T cell receptor structure at 2.5 Å and its orientation in the TCR-MHC complex. *Science*, **274**, 209-219.
- Garboczi, D. N., Ghosh, P., Utz, U., Fan, Q. R., Biddison, W. E. & Wiley, D. C. (1996). Structure of the complex between human T-cell receptor, viral peptide and HLA-A2. *Nature*, **384**, 134-141.
- Garcia, K. C., Degano, M., Pease, L. R., Huang, M., Peterson, P. A., Teyton, L. & Wilson, I. A. (1998). Structural basis of plasticity in T cell receptor recognition of a self peptide-MHC antigen. *Science*, **279**, 1166-1172.
- Ding, Y. H., Smith, K. J., Garboczi, D. N., Utz, U., Biddison, W. E. & Wiley, D. C. (1998). Two human T cell receptors bind in a similar diagonal mode to the HLA-A2/Tax peptide complex using different TCR amino acids. *Immunity*, **8**, 403-411.
- Ding, Y. H., Baker, B. M., Garboczi, D. N., Biddison, W. E. & Wiley, D. C. (1999). Four A6-TCR/peptide/HLA-A2 structures that generate very different T cell signals are nearly identical. *Immunity*, **11**, 45-56.
- Reinherz, E. L., Tan, K., Tang, L., Kern, P., Liu, J. & Xiong, Y. *et al.* (1999). The crystal structure of a T cell receptor in complex with peptide and MHC class II. *Science*, **286**, 1913-1921.
- Degano, M., Garcia, K. C., Apostolopoulos, V., Rudolph, M. G., Teyton, L. & Wilson, I. A. (2000). A functional hot spot for antigen recognition in a superagonist TCR/MHC complex. *Immunity*, **12**, 251-261.
- Hennecke, J., Carfi, A. & Wiley, D. C. (2000). Structure of a covalently stabilized complex of a human  $\alpha\beta$  T-cell receptor, influenza HA peptide and MHC class II molecule, HLA-DR1. *EMBO J.* **19**, 5611-5624.
- Reiser, J.-B., Darnault, C., Guimezanes, A., Gregoire, C., Mosser, T. & Schmitt-Verhulst, A.-M. *et al.* (2000). Crystal structure of a T cell receptor bound to an allogeneic MHC molecule. *Nature Immunol.* **1**, 291-297.
- Wilson, I. A. (1999). Perspectives: protein structure. Class-conscious TCR?. *Science*, **286**, 1867-1868.
- Garcia, K. C., Teyton, L. & Wilson, I. A. (1999). Structural basis of T cell recognition. *Annu. Rev. Immunol.* **17**, 369-397.
- Sim, B. C., Zerva, L., Greene, M. I. & Gascoigne, N. R. J. (1996). Control of MHC restriction by TCR V $\alpha$  CDR1 and CDR2. *Science*, **273**, 963-966.
- Sim, B. C. & Gascoigne, N. R. (1999). Reciprocal expression in CD4 or CD8 subsets of different members of the V $\alpha$ 11 gene family correlates with sequence polymorphism. *J. Immunol.* **162**, 3153-3159.
- Sant'Angelo, D. B., Lucas, B., Waterbury, P. G., Cohen, B., Brabb, T. & Governman, J., *et al.* (1998). A molecular map of T cell development. *Immunity*, **9**, 179-186.
- Fields, B. A., Ober, B., Malchiodi, E. L., Lebedeva, M. I., Braden, B. C. & Ysern, X. *et al.* (1995). Crystal structure of the V $\alpha$  domain of a T cell antigen receptor. *Science*, **270**, 1821-1824.
- Li, H., Lebedeva, M. I., Ward, E. S. & Mariuzza, R. A. (1997). Dual conformations of a T cell receptor V $\alpha$  homodimer: implications for variability in V $\alpha$ V $\beta$  domain association. *J. Mol. Biol.* **269**, 385-394.
- Housset, D., Mazza, G., Gregoire, C., Piras, C., Malissen, B. & Fontecilla-Camps, J. C. (1997). The three-dimensional structure of a T-cell antigen receptor V $\alpha$ V $\beta$  heterodimer reveals a novel arrangement of the V $\beta$  domain. *EMBO J.* **16**, 4205-4216.
- Hare, B. J., Wyss, D. F., Osburne, M. S., Kern, P. S., Reinherz, E. L. & Wagner, G. (1999). Structure, specificity and CDR mobility of a class II restricted single chain T cell receptor. *Nature Struct. Biol.* **6**, 574-581.
- Plaksin, D., Chacko, S., Navaza, J., Margulies, D. H. & Padlan, E. A. (1999). The X-ray crystal structure of a V $\alpha$ 2.6 J $\alpha$ 38 mouse T cell receptor domain at 2.5 Å resolution: alternate modes of dimerization and crystal packing. *J. Mol. Biol.* **289**, 1153-1161.

32. Qadri, A., Radu, C. G., Thatte, J., Cianga, P., Ober, B. T., Ober, R. J. & Ward, E. S. (2000). A role for the region encompassing the c' strand of a TCR V $\alpha$  domain in T cell activation events. *J. Immunol.* **165**, 820-829.
33. Bentley, G., Boulot, G., Karjalainen, K. & Mariuzza, R. (1995). Crystal structure of the  $\beta$  chain of a T cell antigen receptor. *Science*, **267**, 1984-1987.
34. Al-Lazikani, B., Lesk, A. M. & Chothia, C. (2000). Canonical structures for the hypervariable regions of T cell  $\alpha\beta$  receptors. *J. Mol. Biol.* **295**, 979-995.
35. Ciubotaru, M. & Ward, E. S. (1994). Expression of soluble T-cell receptor fragments derived from a T-cell clone associated with murine collagen-induced arthritis. *Immunol. Letters*, **43**, 139-141.
36. Rosloniec, E. F., Brand, D. D., Whittington, K. B., Stuart, J. M., Ciubotaru, M. & Ward, E. S. (1995). Vaccination with a recombinant V $\alpha$  domain of a TCR prevents the development of collagen-induced arthritis. *J. Immunol.* **155**, 4504-4511.
37. Osman, G. E., Toda, M., Kanagawa, O. & Hood, L. E. (1993). Characterization of the T cell receptor repertoire causing collagen induced arthritis in mice. *J. Exp. Med.* **177**, 387-395.
38. Arden, B., Clark, S. P., Kabelitz, D. & Mak, T. W. (1995). Mouse T-cell receptor variable gene segment families. *Immunogenetics*, **42**, 501-530.
39. Kabat, E. A., Wu, T. T., Perry, H. M., Gottesman, K. S. & Foeller, C. (1991). *Sequences of Proteins of Immunological Interest*, US Department of Health and Human Services, Bethesda, MD.
40. Engel, I. & Hedrick, S. M. (1988). Site-directed mutations in the VDJ junctional region of a T cell receptor beta chain cause changes in antigenic peptide recognition. *Cell*, **54**, 473-484.
41. Jorgensen, J. L., Esser, U., Fazekas de St. Groth, B., Reay, P. A. & Davis, M. M. (1992). Mapping T-cell receptor-peptide contacts by variant peptide immunization of single-chain transgenics. *Nature*, **355**, 224-230.
42. Boniface, J. J., Reich, Z., Lyons, D. S. & Davis, M. M. (1999). Thermodynamics of T cell receptor binding to peptide-MHC: evidence for a general mechanism of molecular scanning. *Proc. Natl Acad. Sci. USA*, **96**, 11446-11451.
43. Willcox, B. E., Gao, G. F., Wyer, J. R., Ladbury, J. E., Bell, J. I., Jakobsen, B. K. & van der Merwe, P. A. (1999). TCR binding to peptide-MHC stabilizes a flexible recognition interface. *Immunity*, **10**, 357-365.
44. Garcia, K. C., Radu, C. G., Ho, J., Ober, R. J. & Ward, E. S. (2001). Kinetics and thermodynamics of T cell receptor-autoantigen interactions in murine experimental autoimmune encephalomyelitis. *Proc. Natl Acad. Sci. USA*, **98**, 6818-6823.
45. Mason, D. (1998). A very high level of crossreactivity is an essential feature of the T-cell receptor. *Immunol. Today*, **19**, 395-404.
46. Oldstone, M. B. (1987). Molecular mimicry and autoimmune disease. *Cell*, **50**, 819-820.
47. Gran, B., Hemmer, B., Vergelli, M., McFarland, H. F. & Martin, R. (1999). Molecular mimicry and multiple sclerosis: degenerate T-cell recognition and the induction of autoimmunity. *Ann. Neurol.* **45**, 559-567.
48. Thatte, J., Qadri, A., Radu, C. & Ward, E. S. (1999). Molecular requirements for T cell recognition by a major histocompatibility complex class II-restricted T cell receptor: the involvement of the fourth hypervariable loop of the V $\alpha$  domain. *J. Exp. Med.* **189**, 509-520.
49. Sim, B. C., Wung, J. L. & Gascoigne, N. R. (1998). Polymorphism within a TCRAV family influences the repertoire through class I/II restriction. *J. Immunol.* **160**, 1204-1211.
50. Guex, N. & Peitsch, M. C. (1997). SWISS-MODEL and the Swiss-PdbViewer: an environment for comparative protein modeling. *Electrophoresis*, **18**, 2714-2723.
51. Esnouf, R. M. (1999). Further additions to MolScript version 1.4, including reading and contouring of electron-density maps. *Acta Crystallog. sect. D*, **55**, 938-940.
52. Otwinowski, Z. & Minor, W. (1997). Processing of X-ray diffraction data collected in oscillation mode. *Methods Enzymol.* **276**, 307-326.
53. Wilks, C. M. & Miller, R. (1999). The design and implementation of SnB v2.0. *J. Appl. Crystallog.* **32**, 120-124.
54. Evans, P. R. (1991). The CCP4 program package. In *Crystallographic Computing 5* (Moras, D., Podjarni, A. D. & Thierry, J. C., eds), pp. 136-144, Oxford University Press, Oxford.
55. Jones, T. A., Zou, J. Y., Cowan, S. W. & Kjeldgaard, M. (1991). Improved methods for building protein models in electron density maps and the location of errors in these models. *Acta Crystallog. sect. A*, **47**, 110-119.
56. Brunger, A. T., Adams, P. D., Clore, G. M., DeLano, W. L., Gros, P. & Grosse-Kunstleve, R. W. *et al.* (1998). Crystallography & NMR system: a new software suite for macromolecular structure determination. *Acta Crystallog. sect. D*, **54**, 905-921.
57. Chothia, C., Boswell, D. R. & Lesk, A. M. (1988). The outline structure of the T-cell  $\alpha\beta$  receptor. *EMBO J.* **7**, 3745-3755.

Edited by I. A. Wilson

(Received 25 January 2001; received in revised form 21 May 2001; accepted 22 May 2001)